Investigation of Heat and Moisture Transfer Mechanism in Stone Cultural Relics and Nondestructive Testing Method Based on Infrared Thermography

Zhichao LAI[1], Yingying YANG[1*], Tingting Vogt WU[2,3], Ryad BOUZOUIDJA [2,3], Yue ZHANG[4], Jizhong HUANG[4]

1 School of Energy and Power Engineering, University of Shanghai for Science and Technology, Shanghai, 200093, China

2 Univ. Bordeaux, CNRS, Bordeaux INP, I2M, UMR 5295, F-33400, Talence, France

3 Arts et Metiers Institute of Technology, CNRS, Bordeaux INP, I2M, UMR 5295, F-33400, Talence, France

4 Key Laboratory of Silicate Cultural Relics Conservation (Shanghai University), Ministry of Education, Shanghai 200444, China

* Corresponding author: yangyy741@126.com, 516 Jungong Road, Shanghai, 200093, China.

Abstract

This study conducted water absorption experiments on porous sandstone samples from the Yungang Grottoes. By simultaneously employing Nuclear Magnetic Resonance (NMR) and Infrared Thermography (IRT) techniques acquired both water content distributions along the height direction and surface temperature of sandstone at distinct absorption stages, investigating the spatiotemporal correlation between local extrema of normalized saturation water content change rate and surface temperature gradient. Mathematically, the spatial coordinates of temperature gradient extrema (cm) and normalized saturation water content change rate extrema (cm) exhibit a robust linear relationship. This functional mapping signifies synchronized propagation of thermal and moisture fronts during capillary uptake.

Keywords: Water; Sandstone; Height; Temperature gradient; Saturation

1. Introduction:

Sandstone cultural relics, prevalent worldwide, encompass a vast array of stone carvings, steles, murals, and clay sculptures. These artifacts constitute a vital component of immovable cultural heritage, providing vivid chronicles of historical and artistic evolution [1]. However, in open-air preservation environments, such relics universally exhibit weathering pathologies including powdering, flaking, cracking, and lichen colonization. These deterioration patterns markedly accelerate sandstone degradation, causing irreversible damage to both the aesthetic integrity and intrinsic value of cultural artifacts. Contributing factors encompass temperature-humidity fluctuations, soluble salt crystallization, atmospheric pollutant deposition, and biological activity. Crucially, the adsorption and migration of moisture within natural settings trigger dynamic interactions between porous sandstone and the environment—driving energy transfer and mass exchange that facilitate the translocation and transformation of mineral constituents and inorganic salts (e.g., NaCl). This moisture-driven process represents the predominant degradation mechanism [2]. Consequently, elucidating moisture transport mechanisms within sandstone matrices is imperative for the proactive prevention and accurate diagnosis of cultural relic deterioration.

The loosely packed porous architecture within sandstone facilitates liquid water transport, imparting distinct thermal and hydraulic properties. These properties are intrinsically linked to deterioration processes such as wetting-drying cycles, freeze-thaw cycles, salt dissolution-crystallization, and biotic colonization [3]. Within sandstone, interdependent temperature and moisture fields form a complex coupled system characterized by persistent mass transfer and energy exchange. Under varying environmental conditions, water exists in different phases: gaseous (vapor), liquid, and solid (ice). At given thermodynamic conditions, these phases—predominantly vapor-liquid systems—coexist and maintain dynamic equilibrium through phase transitions [4].

Consolidated evidence confirms that the porosity, pore architecture, and connectivity of sandstone collectively modulate water adsorption-storage characteristics, with saturated water content exhibiting direct proportionality to porosity [5]. Qian et al. [6] employed Water Intrusion Gravimetry (WIG) to quantify moisture distribution, integrating molecular biological analyses with petrophysical and mineralogical characterization techniques. This multidisciplinary approach elucidated synergistic mechanisms by which moisture-pore characteristics govern microbial colonization in heritage sandstone structures.To address lithological variations across regions, Coletti et al. [7] systematically investigated twelve representative building stones from historical structures in Italy, Spain, Greece, and Norway. By integrating mineralogical composition analysis, pore architecture characterization, moisture interaction assessment, and accelerated aging tests, they established a predictive framework for evaluating material susceptibility to decay mechanisms. The results revealed significant disparities in durability and deterioration responses among distinct lithotypes.

The implementation of non-destructive, real-time, and quantitative methodologies for dynamic moisture transport monitoring and assessment within cultural relics is imperative for advancing preventive conservation strategies. Pappalardo et al. [8] employed infrared thermography (IRT) to rapidly detect weathering patterns in natural stone of

historical structures. Using infrared photogrammetry-derived 3D models as a basis, they quantified rock thickness loss induced by mechanical weathering, demonstrating IRT's significant potential as a rapid diagnostic tool for weathering assessment. Regarding moisture front identification, scholars established a quantitative relationship between infrared radiation temperature and moisture content by integrating entropy-based initiation criteria for moisture migration with the first law of thermodynamics, thereby proposing a novel method for detecting moisture migration fronts [9]. For multi-technique nondestructive testing fusion, Fort et al. [10] enhanced the interpretability and feature discrimination of deterioration diagnostics through synergistic analysis of IRT and complementary techniques. Furthermore, by combining IRT with microwave data, they achieved complementary advantages of diverse nondestructive methods, augmented by a convolutional neural network (CNN)-based image fusion approach. This integrated framework significantly improved detection accuracy for moisture-affected zones through combined analysis of temperature anomalies and moisture measurements at varying depths [11].

Current research on moisture migration monitoring and evaluation using infrared thermography (IRT) remains predominantly qualitative. Systematic investigations into the temporal temperature evolution of porous sandstone and the underlying heat and mass transfer mechanisms are still lacking, rendering quantitative assessment challenging. Therefore, it is imperative to quantify the heat and mass transfer processes to establish precise correlations between moisture migration, surface thermal responses, and internal moisture content evolution in porous sandstone. Such quantitative characterization will advance fundamental understanding of heat and mass transfer mechanisms.

This study conducted water absorption experiments on porous sandstone samples from the Yungang Grottoes. By simultaneously employing Nuclear Magnetic Resonance (NMR) and Infrared Thermography (IRT) techniques, we acquired both moisture content distributions along the height direction and surface temperature fields at distinct absorption stages, investigating the spatiotemporal correlation between local extrema of saturated moisture content and surface temperature variation. The methodology comprised four key components:

(1) Temperature gradient analysis: Spatial migration patterns of temperature gradient extrema over absorption time were elucidated through gradient processing of IRT surface data;

(2) Water content normalization: Volumetric water content at each stage was normalized against vacuum-saturated values via NMR, generating normalized saturation curves that revealed spatiotemporal evolution of maximum saturation change rate points;

(3) Bivariate coupling modeling: A robust linear correlation model was established between extrema points of temperature gradient and normalized saturation change rate.

This integrated approach establishes a theoretical framework and practical paradigm for applying IRT to determine absorption duration, localize moisture migration fronts, and predict saturated moisture content profiles in sandstone heritage conservation.

2. Materials and Methods

2.1. Sample Preparation

The Yungang Grottoes (Datong City, Shanxi Province, China) feature medium-to-coarse-grained feldspathic quartz sandstone with tan coloration, interbedded with mudstone and sandy mudstone strata.

As shown in Fig. 1, samples were collected from horizontally extended outcrop sandstone formations adjacent to the heritage site. To mitigate weathering-induced heterogeneity, all specimens were extracted from fresh bedrock >20 cm beneath the rock exterior surface. Using a rock cutting machine, blocks were machined perpendicular to sedimentary bedding into cylindrical specimens Ø35 mm × 70 mm (diameter × height).

Fig. 1. Representative cylindrical specimens of Yungang sandstone

Quantitative characterization of Yungang sandstone's key properties is presented in Table 1:

Table 1. Essential physico-mineralogical properties of Yungang sandstone specimens

Sandstone type	Mineral composition (wt%)	Dry density (g/cm^3)	Porosity (%)

Yungang sandstone	Quartz (62 %)、Calcite (4 %)、Microcline (7 %)、Hematite (1 %)、Clay minerals (27 %)	2.44	8.18

Figure 2 presents the pore size distribution (PSD) curve of Yungang porous sandstone, measured using a high-performance fully automated mercury intrusion porosimeter (AutoPore IV 9620, Micromeritics Instrument Corporation, USA). The PSD curve reveals a unimodal distribution for Yungang sandstone, with the primary peak corresponding to a pore diameter of approximately 0.56 μm. This indicates relatively small pore sizes overall and a relatively narrow distribution range. The ordinate represents the differential distribution of pore volume per unit mass of sandstone with respect to the logarithm of pore diameter.

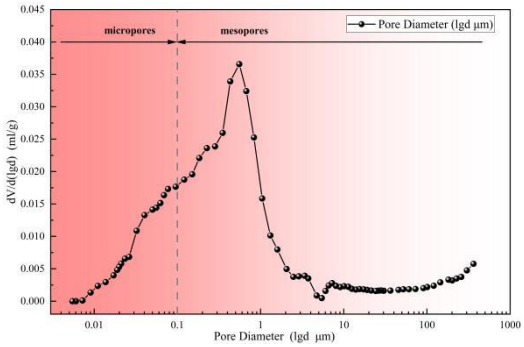

Figure 2. Pore size distribution of Yungang porous sandstone measured by mercury intrusion porosimetry

2.2. Experimental Procedure

The experimental setup and workflow are illustrated in Figure 3. A one-dimensional vertical capillary rise test was conducted on fresh sandstone specimens under controlled laboratory conditions (23 ± 1 °C, 75 ± 5% RH). The procedure consisted of the following steps:

1. A copper wire coil support was placed at the bottom of a flat-bottom glass container. Deionized water was slowly injected until the liquid level reached 2 mm above the support, with the initial position marked;
2. The completely dried sandstone specimen was carefully positioned on the support to initiate capillary absorption, while a timer was simultaneously activated (Note: No direct contact between specimen and container bottom ensured unrestricted water uptake);
3. During testing, the container top was sealed to minimize ambient humidity fluctuations, with deionized water periodically replenished to maintain a constant liquid level;
4. Spatial moisture distribution within the sandstone was monitored non-destructively using nuclear magnetic resonance (NMR) and infrared thermography (IRT). For NMR measurements, specimens were wrapped with plastic film to prevent evaporation, and immediately returned to the container after scanning;
5. The test was terminated when consecutive mass measurements showed variations of less than 1% of the cumulative absorbed water mass, indicating stabilization of capillary absorption.

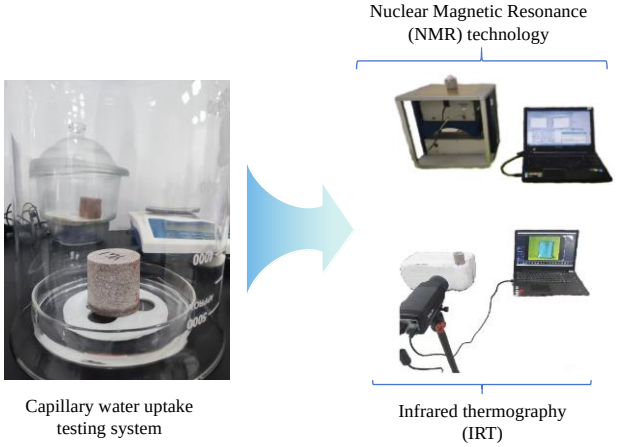

Figure 3. Schematic diagram of the experimental setup and workflow for combined capillary absorption and non-destructive testing (NMR/IRT) in sandstone

2.3. Non-Destructive Testing Equipment

Nuclear Magnetic Resonance (NMR)

Figure 4 displays the spatial distribution of moisture saturation at different time intervals. Stratified water content scanning was performed using a unilateral NMR analyzer (NMR-MOUSE PM25, Magritek GmbH, Germany). Normalized saturation profiles (scale: 0–100 %) were generated by dividing the volumetric water content at each height and time point by the maximum reference value obtained under vacuum-saturated conditions.

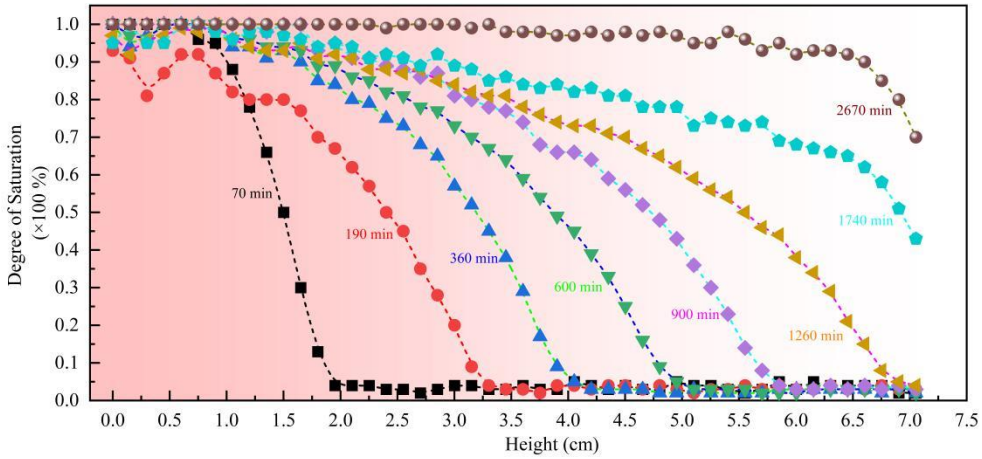

Figure 4. Spatiotemporal evolution of normalized saturation during capillary absorption in sandstone obtained by NMR

Infrared Thermography (IRT)

Surface temperature fields were acquired using an infrared camera (FLIR A615, FLIR Systems Inc., USA). The system features an uncooled focal plane array detector with 640 × 480 pixel resolution, operating in the temperature range of -20 to 150 ℃. The measurement accuracy meets ±2 ℃ or ±2% of reading (whichever is greater). Following the manufacturer's protocol, the sandstone surface emissivity was set to 0.94, with a constant perpendicular distance (30 cm) maintained between the lens and specimen surface. Raw thermograms were processed via FLIR Tools+ software for temperature field reconstruction and quantitative analysis.

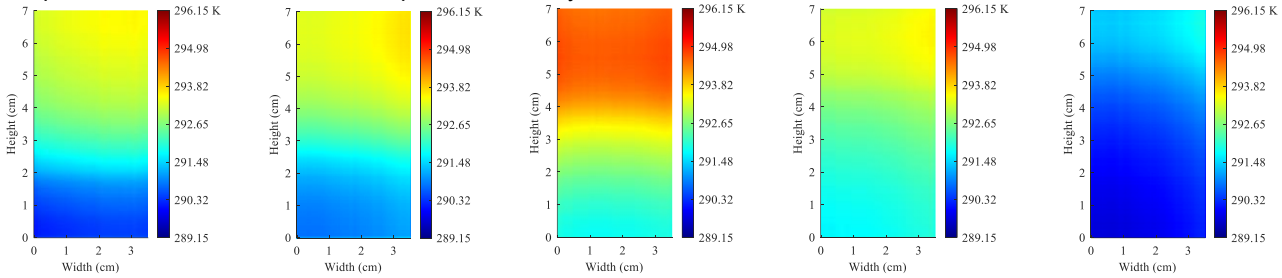

(a) 70min *(b) 190min* *(c) 60min* *(d) 600min* *(e) 900min*

Figure 5. Spatiotemporal evolution of surface temperature fields during capillary absorption in sandstone captured by infrared thermography

3. Results and Discussion

3.1. Spatiotemporal Evolution of Thermal Fields

Non-contact thermal monitoring was performed using the FLIR A615 infrared camera. Along the central symmetry axis of the 70-mm-high sandstone specimen, a linear measurement path was discretized into 48 equally spaced nodes. Temperature data extracted at these nodes enabled digital reconstruction of thermal profiles with a spatial resolution of 1.46 mm/node.

The temperature gradient method enables high spatiotemporal resolution characterization for coupled heat-moisture transfer processes, providing refined quantification of microscale transport phenomena and real-time resolution of dynamic evolution patterns [12]. Whereas conventional macroscopic temperature measurements (e.g., bulk temperature monitoring) merely reflect the global thermal state of porous media with vulnerability to environmental interference, the gradient approach significantly enhances spatial resolution through differential operations that extract physical quantity gradients. This methodology effectively suppresses common-mode noise via discrete differentiation. By correlating the maxima of temperature variation rates with moisture migration fronts, this technique demonstrates superior sensitivity and spatial resolution over traditional macroscopic methods, allowing precise quantification of moisture-temperature coupling mechanisms [13].

In this study, the porous sandstone sample absorbed water from its base. Experimental temperature data revealed an overall increasing temperature trend along the height direction. However, within regions exhibiting significant moisture

migration, a pronounced temperature decrease was observed. As the porous sandstone constitutes a continuous medium, heat conduction driven by temperature differences coexists with the moisture migration process. The direction of the resultant heat flux is always opposite to the temperature gradient.

For temperature data processing, a hybrid algorithm integrating the Piecewise Cubic Hermite Interpolating Polynomial (PCHIP) with moving average filtering was employed. This approach effectively prevents the generation of spurious extrema by preserving local monotonicity. Its shape-preserving property ensures an optimal balance between the smoothness of the fitted curve along the height direction and its physical plausibility. Concurrently, the application of moving average filtering efficiently suppresses measurement noise. To facilitate the clear presentation of findings regarding temperature variation patterns, the absolute value of the temperature gradient was adopted.

Figure 6 depicts the variations in surface temperature difference and temperature gradient along the height direction of the porous sandstone sample at different water absorption times. The experimental data points and the corresponding fitted curves are superimposed in the figure.

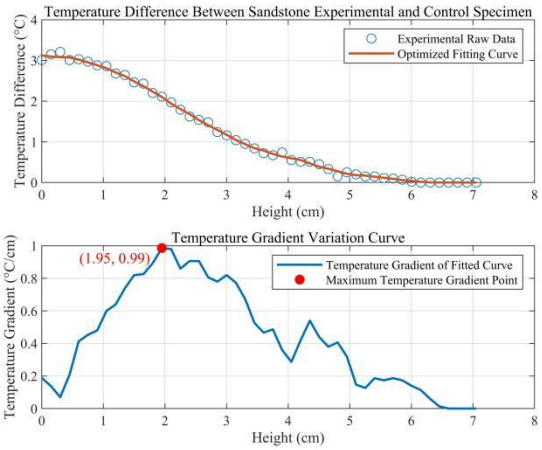

(a) 70min

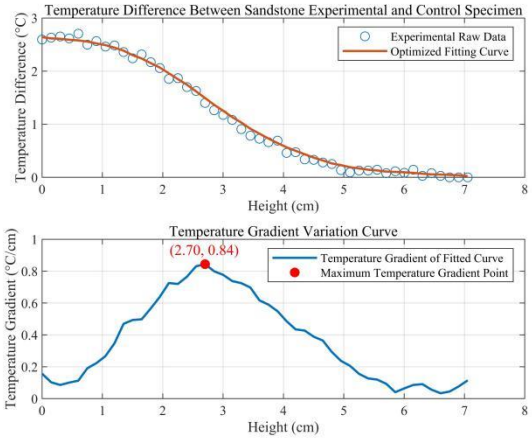

(b) 190min

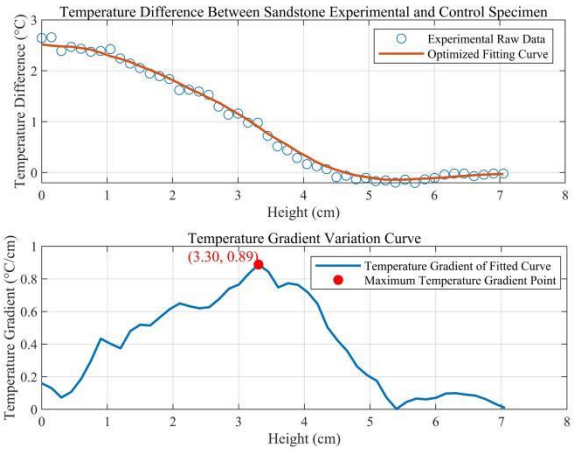

(c) 360min

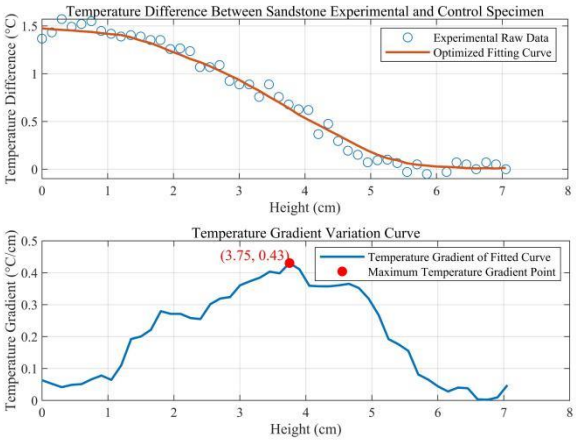

(d) 600min

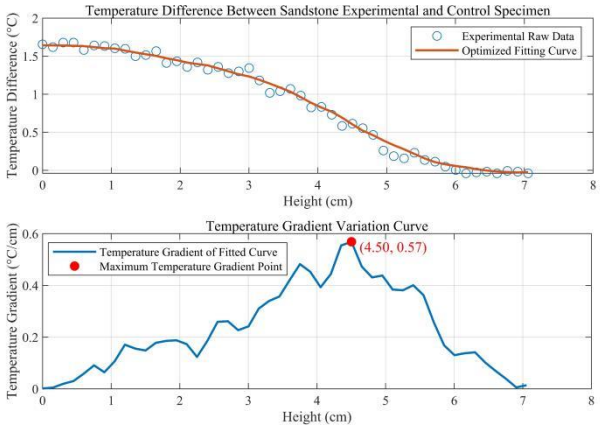

(e) 900min

Figure 6: Variations in Surface Temperature Difference and Temperature Gradient along the Height Direction of the Porous Sandstone Sample at Different Water Absorption Times

Figure 7 illustrates the temporal evolution of the peak temperature gradient height. Experimental data demonstrate a strong linear relationship (correlation coefficient $R^2 = 0.95$) between the height of the temperature gradient extremum and water absorption duration.

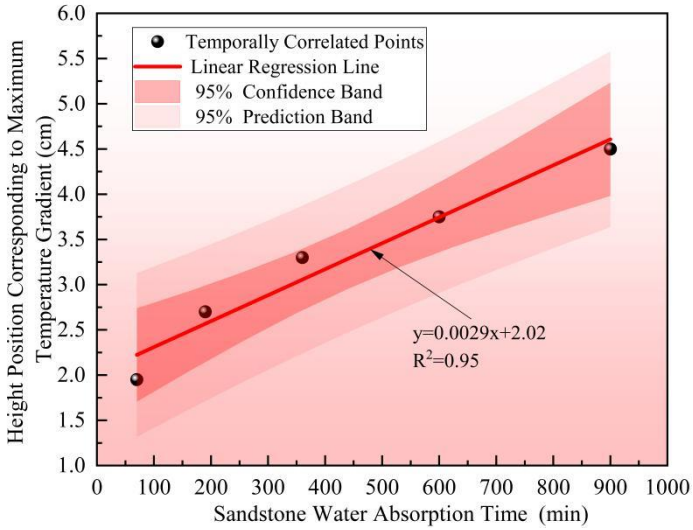

Figure 7: Linear Evolution of Peak Temperature Gradient Height versus Water Absorption Time in Porous Sandstone

3.2. Spatiotemporal Distribution of Normalized Water Saturation

Volumetric water content of porous sandstone under vacuum-saturated conditions and during water absorption was quantified via nuclear magnetic resonance (NMR) measurements. Normalized saturation profiles (range: 0-100%) were generated by scaling the height-dependent volumetric water content at each time increment against the maximum value at vacuum saturation. This normalization approach provides two critical advantages: (1) elimination of interference from pore structure heterogeneity, and (2) enhanced visualization and mechanistic interpretation of wetting front dynamics. Compared to absolute water content data, the normalized profiles suppress local anomalies and demonstrate superior suitability for theoretical model validation [14].

Figure 8 depicts the spatiotemporal evolution of normalized water saturation and its rate of change during water absorption. Data processing employed the hybrid PCHIP-moving average algorithm described. The piecewise cubic Hermite interpolating polynomial (PCHIP) preserves local monotonicity to eliminate spurious extrema, while its shape-preserving property ensures optimal balance between curve smoothness and physical plausibility along the height direction. Concurrent moving average filtering suppresses measurement noise. Absolute values of saturation change rates were adopted to clarify variation trends. Experimental results are presented in Figure 8..

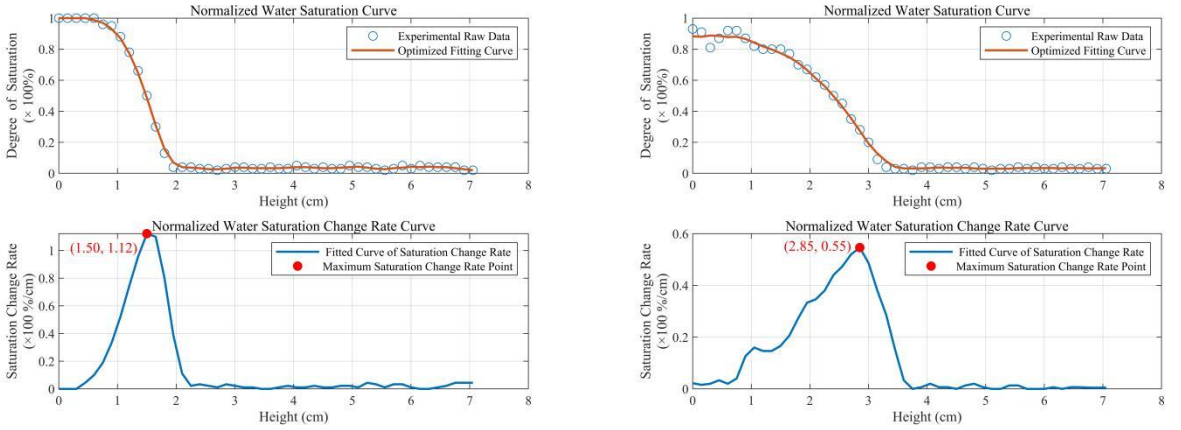

(a) 70min

(b) 190min

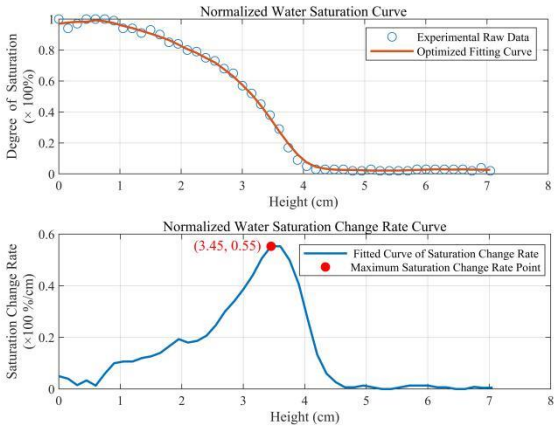

(c) 360min

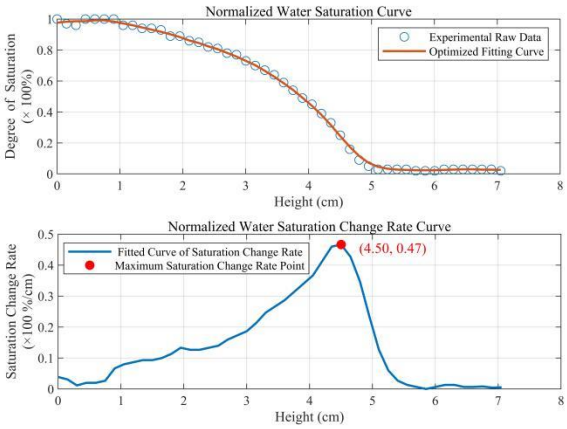

(d) 600min

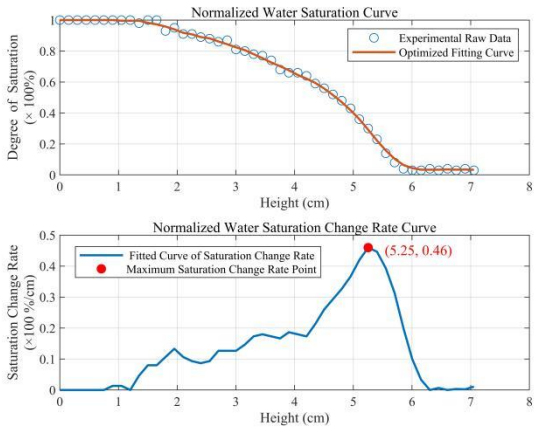

(e) 900min

Figure 8: Spatiotemporal Evolution of Normalized Water Saturation and Its Change Rate along the Height Direction during Water Absorption in a Porous Sandstone Sample

Figure 9: Linear Evolution of Extremum Points in Normalized Water Saturation Change Rate versus Water Absorption Time.Experimental data reveal a strong linear correlation (R^2 = 0.91) between the height position of the change rate extremum in fitted saturation profiles and water absorption duration, with the evolutionary trend depicted in Figure 9.

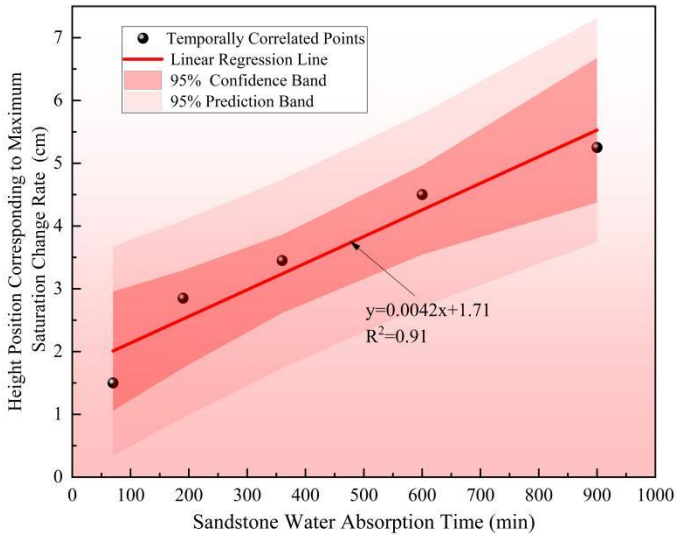

Figure 9: Linear Evolution of Extremum Points in Normalized Water Saturation Change Rate versus Water Absorption Time

3.3. Theoretical Modeling and Experimental Principles of Heat-Mass Transfer in Porous Sandstone

The spatial correlation between extrema of temperature gradient and extrema in the rate of change of saturation moisture content during heat-mass transfer necessitates coupled solutions of thermo-hydraulic diffusion equations. The theoretical framework incorporates the following postulates:

1. Moisture flux is proportional to the moisture content gradient, with non-Darcian effects (e.g., inertial terms or non-Newtonian behavior) neglected;
2. Isotropic homogeneous medium with constant effective thermal conductivity λ and moisture diffusivity $D(\theta)$;
3. Conductive and latent heat transfer dominate, while convective heat transfer is negligible ;
4. Uni-dimensional transport along the vertical axis, excluding transverse diffusion and boundary interactions ;
5. Instantaneous latent heat release/absorption, omitting phase-change kinetics and thermal radiation
6. Temporally invariant wetting front velocity during extremum point analysis.

The governing equations are coupled as follows:

Energy conservation equation and moisture diffusion equation:

$$\rho c_p \frac{\partial T}{\partial t} = \nabla \cdot (\lambda \nabla T) - \rho_w L_v \frac{\partial \theta}{\partial t} \tag{2}$$

$$\frac{\partial \theta}{\partial t} = \frac{\partial}{\partial z}\left(D(\theta) \frac{\partial \theta}{\partial z} \right) = D(\theta) \frac{\partial^2 \theta}{\partial z^2} \tag{3}$$

λ thermal conductivity (*W/(m·K)*), ρ_w water density (*kg/m³*), L_v latent heat of vaporization (kJ/kg), θ volumetric moisture content (%), $D(\theta)$ moisture diffusivity (*m²/s*)—treated as constant in this study.

This equations reveal inherent coupling between thermal and moisture transfer fields:

$$\rho_w L_v \frac{\partial \theta}{\partial t} = \lambda \frac{\partial^2 T}{\partial z^2} - \rho c_p \frac{\partial T}{\partial t} \tag{4}$$

At the extremum of moisture content variation rate:

$$\frac{\partial^2 \theta}{\partial z^2} = 0 \tag{5}$$

Substituting into the moisture transport equation (Eq. 3) yields:

$$\frac{\partial \theta}{\partial t} = D(\theta) \cdot \frac{\partial^2 \theta}{\partial z^2} = D(\theta) \cdot 0 = 0 \tag{6}$$

The zero temporal derivative of moisture content indicates dynamic equilibrium between moisture flux and evaporation loss, resulting in instantaneous stabilization of the wetting front. This state reflects a thermal equilibrium where latent heat release balances conductive heat diffusion, ($\partial T/\partial t = 0$)。

The coupled thermo-hydraulic equation (Eq. 4) reduces to:

$$0 = \rho_w L_v \frac{\partial \theta}{\partial t} = \lambda \frac{\partial^2 T}{\partial z^2} - \rho c_p \frac{\partial T}{\partial t} = \lambda \frac{\partial^2 T}{\partial z^2} - 0 \tag{7}$$

Derivation yields the characteristic relation:

$$\frac{\partial^2 T}{\partial z^2} = 0 \tag{8}$$

The fulfillment of Eq. (8) at temperature gradient extrema confirms spatial coincidence with water content gradient extrema, demonstrating strong inherent thermo-hydraulic coupling. This theoretical finding remains subject to the idealized assumptions.

Fig. 10. Linear correlation of heat-mass transfer in porous sandstone: Experimental evidence unequivocally reveals a statistically significant linear spatial distribution (R^2 = 0.98) between normalized water saturation variation rate extrema and temperature gradient extrema.

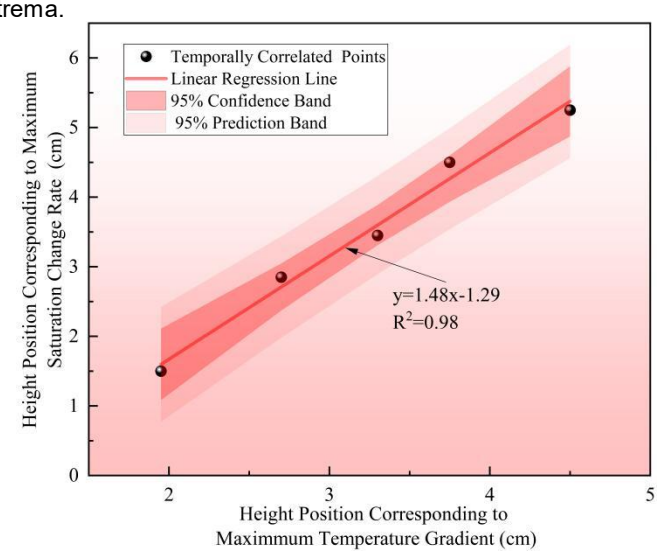

Fig. 10. Linear correlation of heat-mass transfer in porous sandstone

In the in-situ detection of porous sandstone relics, infrared non-destructive testing equipment offers advantages of operational convenience and lower cost for temperature field measurements, whereas nuclear magnetic resonance (NMR) equipment for measuring saturated water content is prohibitively expensive and unsuitable for field applications. By establishing a linear relationship between the extremum points of temperature gradient and normalized water saturation variation rate , the extremum points of the normalized saturation water content can be inferred from temperature data acquired by infrared devices during in-situ inspections. This approach enables precise localization of the wetting front position. The aforementioned research provides valuable insights for quantifying heat and mass transfer phenomena in porous sandstone relics and facilitates in-situ moisture content detection.

The revealed spatiotemporal distribution patterns of linear variations in temperature gradient extrema and normalized saturation water content change rate extrema at distinct time intervals, along with their established linear correlation, provide critical foundations for quantitative analysis of heat-mass transfer in porous sandstone during in-situ monitoring. This methodology further enables precise localization of wetting front propagation zones.

4. Conclusions

1.The differential thermal analysis method enhances spatial resolution and suppresses common-mode noise through gradient operations. Quantitative analysis reveals a linear dependence between capillary absorption time (min) and the height of temperature gradient extrema (cm) during 0-900 min:

2.Normalized saturation profiles mitigate pore-structure heterogeneity and eliminate local anomalies. The height of normalized saturation water content change rate extrema (cm) follows a linear function of absorption time (min):

3.Mathematically, the spatial coordinates of temperature gradient extrema (cm) and normalized water content change rate extrema (cm) exhibit a robust linear correspondence:This functional mapping signifies synchronized propagation of thermal and moisture fronts during capillary uptake. The deviation suggests a slight hysteresis in wetting front advancement, attributable to latent heat effects during phase change.

REFERENCES

[1] Zhang Y, Zhang Y, Huang J. Experimental study on capillary water absorption of sandstones from different grotto heritage sites in China[J]. Heritage Science, 2022, 10(1): 25.

[2] Huang J, Zheng Y, Li H. Study of internal moisture condensation for the conservation of stone cultural heritage[J]. Journal of Cultural Heritage, 2022, 56: 1-9.

[3] Hu J, Huang J, Cheng Y. Experimental study evaluating the performance of thermal conductivity prediction models for air–water saturated weathered sandstone heritage[J]. Heritage Science, 2024, 12(1): 366.

[4] Shen Y, Liang C, Steiger M, et al. Quantitative analysis on the impact factors of salt weathering for sandstone grottoes along Silk Road, China[J]. Journal of Cultural Heritage, 2024, 67: 522-533.

[5] Feng C, Janssen H. Hygric properties of porous building materials (VII): Full-range benchmark characterizations of three materials[J]. Building and Environment, 2021, 195: 107727.

[6] Qian Y, Lang-Yona N, Hu P, et al. Water characteristics and retention in Angkor sandstone monuments and their linkage with microorganisms responsible for ammonia oxidation and nitrate accumulation[J]. Science of The Total Environment, 2025, 969: 178636.

[7] Coletti C, Antonelli F, Germinario L, et al. Investigating stone materials from some European cultural heritage sites for predicting future decay[J]. Rendiconti Lincei. Scienze Fisiche e Naturali, 2025, 36(1): 103-127.

[8] Pappalardo G, Mineo S, Caliò D, et al. Evaluation of Natural Stone Weathering in Heritage Building by Infrared Thermography[J]. Heritage, 2022, 5(3): 2594-2614.

[9] Zhang F, Zhang X, Li Y, et al. Quantitative description theory of water migration in rock sites based on infrared radiation temperature[J]. Engineering Geology, 2018, 241: 64-75.

[10] Fort R, Feijoo J, Varas–Muriel M J, et al. Appraisal of non-destructive in situ techniques to determine moisture- and salt crystallization-induced damage in dolostones[J]. Journal of Building Engineering, 2022, 53: 104525.

[11] Wang F, Huang J, Fu Y. Convolutional neural network-based multimodal image information fusion for moisture damage assessment of cultural heritage buildings[J]. Measurement, 2025, 242: 115972.

[12] Kumar A, Bidarmaghz A, Khoshghalb A, et al. Coupled heat and moisture migration in unsaturated soils subjected to thermal gradients[J]. Computers and Geotechnics, 2025, 177: 106893.

[13] Wu T, Zhan L, Feng S, et al. Numerical analysis of moisture and gas transport in earthen final covers considering effects of vapor and temperature gradient[J]. Soils and Foundations, 2023, 63(1): 101262.

[14] Wang C, Yang Y L, Cai G, et al. Improvement of normalized prediction model of soil thermal conductivity[J]. International Communications in Heat and Mass Transfer, 2024, 157: 107792.